Available online at www.sciencedirect.com
SCIENCE DIRECT®
International Journal of Thermal Sciences 43 (2004) 541–554
International Journal of Thermal Sciences
www.elsevier.com/locate/ijts

Non-equilibrium theories for macroscale heat transfer: ablative composite layer systems

N. Puiroux, M. Prat, M. Quintard *

Institut de mécanique des fluides de Toulouse, allée du professeur Camille Soula, 31400 Toulouse, France

Received 16 July 2003; accepted 27 November 2003

Available online 13 February 2004

Abstract

An original model describing non-equilibrium heat transfer in ablative composite layers has been studied. The model is obtained as an extension of previous work involving the use of the volume averaging method to upscale the micro-scale equations. Using this methodology, it is shown that non-equilibrium models existing in the literature may lead to equilibrium conditions for typical aerospace applications. The new model presented in this paper takes into account two separate macro-scale "phases", but, contrary to previous models, they are constituted of the inert part of the material, on one side, and the mixture of gas and pyrolysable part of the material on the other side. The theoretical development allows to estimate the transport properties in the macro-scale model from micro-scale unit cell characteristics. They are obtained for different types of unit cells: simple stratifed unit cells, and unit cells characteristic of woven composites. Quantitative indications are given for the estimates of the macro-scale thermal diffusivity tensors, and for the volume heat exchange coefficient.

1. Introduction

Rocket design requires a thorough knowledge of the thermal processes during a liftoff. In this paper, we are particularly interested in the thermal behavior of the ablative composite layers used to protect the nozzle. The objective of this protection is to prevent the external wall of the nozzle from reaching a critical temperature. The principle of this thermal protection is simple: endothermic chemical reactions within the material are used to slow down the progression of the heat front. The composite material is composed of two phases: resin and carbon fiber. During a liftoff, the resin is pyrolysed and transformed into an inert phase (called coke) and a gas phase. The carbon fibers do not participate in the chemical reactions and do not undergo transformations under the effect of heat. A schematic picture of the different phases and scales involved in the description of the ablative layers is represented in Fig. 1, where we have figured three scales of interest, namely the sub-microscopic scale (V_{s-m}), the microscopic scale (V) and the composite scale. At the sub-microscopic scale, we can separate the gas and the resin phases. At the microscopic scale, we can distinguish two "phases": a indicating the active pseudo-phase and i indicating the carbon fibers. The active pseudo-phase itself is a porous medium composed of gas, indicated by g, and resin or coke, noticed p. We remind that the chemical reactions affect both the resin and the gas phase, and that they lead to porosity variations with time. At the composite scale, we want to consider the composite as an homogeneous media with characteristics taking into account the microscopic structure.

A typical problem for this study is described on Fig. 2. We consider a part of the ablative composite layers which covers the booster nozzle of a "typical" rocket. This work has been undertaken in the framework of constraints with the French aerospace industry. While sensitive material is covered by industrial secret, the problem studied in this paper is generic and therefore will not be illustrated by specific data. At the initial time, we consider that the temperature of the composite and the pressure of gas are uniformly constant. At the ignition of the boosters, maintained constant heat flux is supplied at the layer surface, and the pressure is a constant valuer over this surface. We do not take into account, in this paper, the expansion or the ablation of the composite.

Many studies have been performed in order to optimally design these protective layers. They are based on a descrip-

* Corresponding author.
E-mail addresses: nicolas.puiroux@imft.fr (N. Puiroux), marc.prat@imft.fr (M. Prat), michel.quintard@imft.fr (M. Quintard).

1290-0729/$ – see front matter © 2004 Elsevier SAS. All rights reserved.
doi:10.1016/j.ijthermalsci.2003.11.004

Nomenclature

a	coefficient of the relation between Nusselt number and Reynold number	
$a_v h$	heat transfer coefficient	$W{\cdot}m^{-3}{\cdot}K^{-1}$
b	coefficient of the relation between Nusselt number and Reynold number	
$\mathbf{b}$	closure mapping vector	m
c	specific heat	$J{\cdot}kg^{-1}{\cdot}K^{-1}$
h	enthalpy	$J{\cdot}kg^{-1}$
δH	difference of enthalpy	$J{\cdot}kg^{-1}$
$\mathbf{K}$	permeability	m^2
l	characteristic length	m
$\mathbf{l}$	position vector	m
ℓ	characteristic length between fibers	m
L	domain characteristic length	m
$\mathbf{n}$	unit normal vector	
Nu	Nusselt number	
P	pressure	Pa
Pe	Peclet number	
q''	heat of decomposition	$J{\cdot}kg^{-1}$
r_0	radius of the averaging volume V_n	m
R_0	radius of the averaging volume V	m
Re	Reynold number	
s	closure mapping scalar	
T	temperature	K
$\mathbf{v}$	averaged gas-phase interstitial velocity, r_0 scale	$m{\cdot}s^{-1}$
$\mathbf{V}$	averaged gas-phase interstitial velocity, R_0 scale	$m{\cdot}s^{-1}$
V	averaging volume at Darcy-scale	m^3
V_{s-m}	averaging volume at sub-microscopic scale	m^3

Greek letters

$\delta_{\alpha\beta}$	Croneker symbol	
ε	volume fraction, r_0 scale	
λ	effective thermal conductivity	$W{\cdot}m^{-1}{\cdot}K^{-1}$
μ	viscosity	$kg{\cdot}m^{-1}{\cdot}s^{-1}$
ξ_p	rate of pyrolysis	
ρ	density	$kg{\cdot}m^{-3}$
ϕ	volume fraction, R_0 scale	

Subscript

a	relative to the active part of the material
g	relative to gas
i	relative to the inert part of the material
p	relative to the pyrolysable part of the material
s	relative to the material
$\overline{\overline{=}}$	tensorial notation

Superscript

$\tilde{}$	deviation quantity

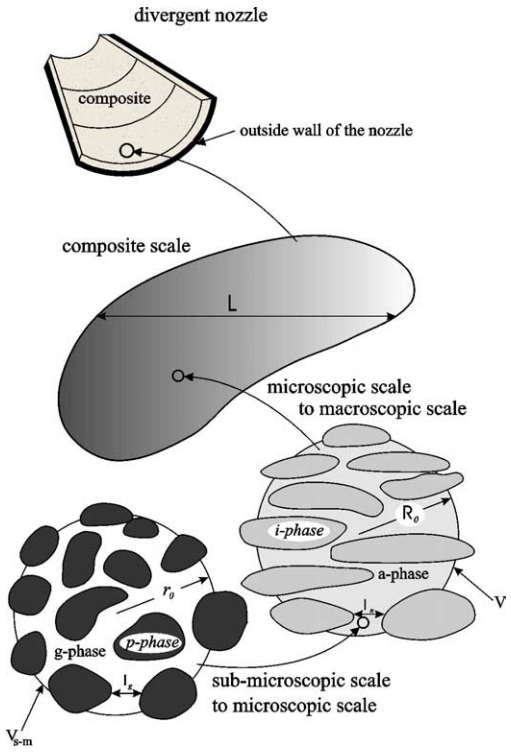

Fig. 1. Different scales in the composite layer.

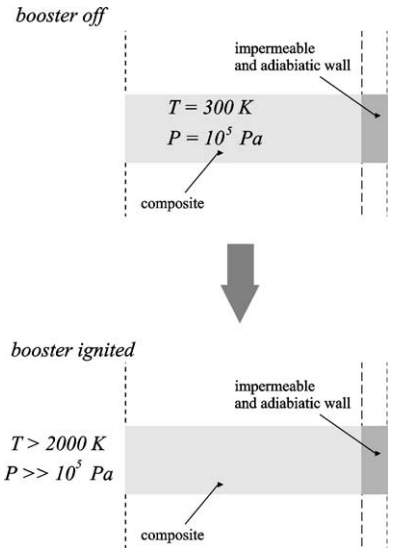

Fig. 2. Reference problem for heat transfer in ablative composite layers.

tion of the heat transfer processes in terms of macro-scale models [1–4]. We can classify these studies in two categories. In the first one, the authors [1–3] consider *local thermal equilibrium processes*, i.e., the macro-scale model at the composite scale involves a single continuum describing the macro-scale behavior of the phase mixture. To be clear, they

do not make distinctions between the macro-scale temperatures of the gas phase, the resin phase and the fiber phase. These models tend to underestimate the temperature for conditions corresponding to rocket liftoff [3,4]. Indeed gaps between experimental simulations and numerical simulations have been observed for a typical liftoff problem. In the second category of models, the authors [1,4] consider the possible existence of local thermal non-equilibrium processes, i.e., macro-scale phases have different temperatures at the composite scale. However, all papers consider the two following macro-scale phases: a composite phase made of all micro-scale solid phases, and a gas phase. In this paper, the relevance of these models for the physical applications which is of interest for us is discussed based on quantitative arguments.

It is found that these models would lead to very negligible difference between the two macro-scale temperatures. The major argument supporting the emergence of local-equilibrium conditions in these previously published local non-equilibrium models is that the characteristic length-scale corresponding to the separation of the gas-phase with the other phases, ℓ_g, is rather small, let us say one order of magnitude smaller than the distance between fibers, ℓ (Fig. 1). Since the heat exchange coefficient varies with the inverse of the square of this characteristic length (Quintard and Whitaker [5]), i.e., ℓ_g^{-2}, it is large enough for the model to produce local-equilibrium conditions. The idea, behind the original model proposed in this paper, is that the mechanism that could lead to non-equilibrium is not the heat transfer between the resin and the gas phase, but, rather, the conduction of heat between the resin and the fibers with a typical heat exchange coefficient this time on the order of ℓ^{-2}, i.e., several orders of magnitude lower than for the previous models. This model is developed as follows:

- The resin and the gas phases have the same macro-scale temperature at the composite scale. The associated macro-scale continuum is called the *active pseudo-phase* by reference to the existence of the pyrolysis phenomenon.
- A macro-scale temperature is also associated to the carbon fiber phase. The corresponding continuum is called *inert phase*.

The resin and the gas form a porous medium, with a relatively small pore-scale, which is consistent, as indicated above, with the use of a local thermal equilibrium model. Therefore, the ablative composite is a particular porous medium composed of an impermeable inert phase (carbon fibers) and of a permeable active pseudo-phase (gas and resin), which is itself described as a porous medium at an intermediate, smaller, scale. The behavior at the composite scale of this material can be described by averaged equations, and they are introduced in this paper by extension of previous results obtained for usual porous media by a volume averaging approach. Details about the method are given in the paper. As usual, the relationship between the two involved scales gives several closure problems that may be used to estimate the macro-scale transport properties from the small-scale characteristics. They are solved in this paper for different unit cells relevant for the problem of composite material under consideration.

2. Existing models

In this section, we review the different models existing in the literature. We start with a discussion of classical macro-scale energy balance equations, and then review how these ideas have been applied to the pyrolysis of ablative layers.

Passive heat transfer has been the object of many studies in the literature, especially in the case of two phases. The fundamental discussions focus on the problem of *local-thermal equilibrium* or *local thermal non-equilibrium* [5–11]. If the diffusivity of the two phases is close enough, local thermal equilibrium takes place and a single macro-scale equation can be written involving an effective diffusion tensor. Otherwise, special treatment is needed to handle local non-equilibrium conditions. In this case, a large place has been devoted in the literature to the development of two-equation models for averaged temperatures associated to the two different phases. The case of reactive heat transport in porous media has received less attention. From a theoretical point of view, heat sources due to chemical reactions can be incorporated easily through simple averages in the one-equation model associated with local equilibrium, while, on the contrary, this requires more work in the case of two-equation models [12]. In this latter paper, heat sources where considered as constants, and no special coupling with the mass balance equations was considered. A more detailed analysis of reactive transport in porous media, and the associated macro-scale models, can be found in [13,14].

We retain from this brief review that two major classes of macro-scale models can be developed depending on the assumption made about local thermal equilibrium. Concerning the macroscopic description of ablative layer pyrolysis, we found the same types of models. Most authors [1–3] use local thermal equilibrium models. Some authors, however, like Kansa et al. [1] and Florio et al. [4] have considered local thermal non-equilibrium models. These different models are discussed in the next section.

First, we briefly describe the different balance equations for the local thermal equilibrium model and for the non-equilibrium models. Then we discuss the significance of those models for conditions corresponding to rocket liftoff. We do not present here in detail the pyrolysis models and the various correlations used for the different parameters, since this is not necessary due to the assumptions made for the upscaling problem described later in this paper.

2.1. Local thermal equilibrium models

Given the complexity of the material and processes involved, it is not surprising to find many different models. We will present only three different models that are representative of the major classes of model developed so far. The first one has been developed by Kansa et al. [1] in the objective to model wood combustion. The second one has been written by Darmon and Balageas [2] for modeling heat and mass transfer in pyrolysable composites. The last one has been written by Henderson and Wiecek [3] who have studied the thermally-induced response of decomposing, expanding polymer composites. Since the objective of this paper is to discuss the relevance of thermal models, we present their results without the effects of material decomposing and expanding. This restriction is very important since it simplifies a lot the different equations of the model, in particular it will suppress terms associated with pore-scale interface velocity. Henderson and Wiecek [3] and Florio et al. [4] suggest a model to solve the variation of the control volume width in taking into account the temperature, the density of the solid, the volume fraction and the rate of pyrolysis. Of course, strong couplings appears in the different balance equations.

2.1.1. Mass balance equation

The mass balance equation for the gas phase is written in all the models as

$$\frac{\partial \phi \rho_g}{\partial t} + \nabla \cdot (\phi \rho_g \mathbf{V}_g) = -\frac{\partial (1-\phi)\rho_s}{\partial t} \tag{1}$$

with $\frac{\partial (1-\phi)\rho_s}{\partial t}$ being the density variation of the solid phase per unit volume due to the pyrolysis and ϕ the volume fraction. Here, "solid phase" refers to all solid phases introduced in the detailed description presented in the introduction.

In most models used for this rocket application, an "equivalent" gas is considered [1,4]. "Equivalent" means that a single mass balance equation is written instead of a system of equations corresponding to the various components of the gas mixture. We do not discuss this simplification here, since it is irrelevant for our discussion about the heat transfer models.

2.1.2. Momentum balance equation

Most authors neglect the inertia term in the momentum balance equation, so it takes the form of Darcy's law:

$$\phi \mu_g \mathbf{K}^{-1} \cdot \mathbf{V}_g + \nabla P = \mathbf{0} \tag{2}$$

It must be noticed that gravity has been neglected in this problem.

2.1.3. Energy balance equation

Kansa et al. [1] write the energy balance equation as:

$$\big(\phi \rho_g c_g + (1-\phi)\rho_s c_s\big)\frac{\partial T}{\partial t} + \phi \rho_g c_g \mathbf{V}_g \cdot \nabla T - \frac{\partial \phi P}{\partial t} + (h_R + h_s - h_g)\frac{\partial (1-\phi)\rho_s}{\partial t} - \nabla \cdot \big(\underline{\underline{\lambda}}^* \cdot \nabla T\big) = 0 \tag{3}$$

with

$$\underline{\underline{\lambda}}^* = \phi \underline{\underline{\lambda}}_g + (1-\phi)\underline{\underline{\lambda}}_s \tag{4}$$

Henderson and Wiecek [3] write this equation in neglecting the term $\frac{\partial \phi P}{\partial t}$ which expresses the gas work:

$$\big(\phi \rho_g c_g + (1-\phi)\rho_s c_s\big)\frac{\partial T}{\partial t} + \phi \rho_g c_g \mathbf{V}_g \cdot \nabla T + (h_R + h_s - h_g)\frac{\partial (1-\phi)\rho_s}{\partial t} - \nabla \cdot \big(\underline{\underline{\lambda}}^* \cdot \nabla T\big) = 0 \tag{5}$$

Darmon and Balageas [2] have introduced an additional complexity by separating all the species which constitute the gas:

$$\big(\phi \rho_g c_g + (1-\phi)\rho_s c_s\big)\frac{\partial T}{\partial t} + \sum_i \big(\hat{\rho}_{g,i} c_{g,i} \mathbf{V}_{g,i}\big) \cdot \nabla T + (h_s - h_g)\frac{\partial (1-\phi)\rho_s}{\partial t} + \sum_i \big(h_i \nabla \cdot (\rho_{g,i} \mathbf{V}_{g,i})\big) - h_g \nabla \cdot (\rho_g \mathbf{V}_g) - \nabla \cdot \big(\underline{\underline{\lambda}}^* \cdot \nabla T\big) = 0 \tag{6}$$

with

$$\underline{\underline{\lambda}}^* = \underline{\underline{\lambda}}_g^{\phi} \cdot \underline{\underline{\lambda}}_s^{1-\phi} \tag{7}$$

It must be noticed that Eqs. (4) and (7) represents estimates of the effective thermal conductivities, as classically used in chemical engineering. The first one corresponds to the upper Wiener's bound for the effective conductivity of two-phases material [15], and the second has been justified by Matheron [16] for randomly distributed conductive two phases in two dimensions. As will be shown later, these estimates can be improved by solving the closure problems associated to upscaling theories, provided some details are known about the micro-scale structure [17]. Such closure problems will be given for the problem under consideration in this paper in the last section.

2.2. Local thermal non-equilibrium models

To our knowledge, there are only two papers in the literature that describe local thermal non-equilibrium models for such materials. The frst one is found in Kansa et al. [1]. The second one is due to Florio et al. [4]. This latter paper is focused on the impact of the assumption of local thermal equilibrium on the overall thermally induced response of a composite.

In this section we present only the energy balance equations, since the mass balance equations and the momentum balance equations are unchanged in all these models.

2.2.1. Energy balance equations

In both papers, the authors consider that the composite, i.e., all the solid phases, and the gas, have different temperatures at the composite-scale. We will discuss this choice later. Kansa et al. [1] write the energy balance equation for the gas phase as

$$\phi\rho_g c_g \frac{\partial T_g}{\partial t} + \phi\rho_g c_g \mathbf{V}_g \cdot \nabla T_g - \frac{\partial \phi P}{\partial t} - \frac{a_v h}{\phi}(T_s - T_g) - \nabla \cdot (\underline{\underline{\lambda}}_g \cdot \nabla T_g) - h_g \frac{\partial (1-\phi)\rho_s}{\partial t} + q_g'' = 0 \tag{8}$$

and for the solid phase

$$(1-\phi)\rho_s c_s \frac{\partial T_s}{\partial t} + \frac{a_v h}{1-\phi}(T_s - T_g) - \nabla \cdot (\underline{\underline{\lambda}}_s \cdot \nabla T_s) - h_s \frac{\partial (1-\phi)\rho_s}{\partial t} + q_s'' = 0 \tag{9}$$

Florio et al. [4] do not neglect the source of kinetic energy in the gas phase due to pyrolysis, and therefore write the energy balance equation for the gas phase as

$$\phi\rho_g c_g \frac{\partial T_g}{\partial t} + \phi\rho_g c_g \mathbf{V}_g \cdot \nabla T_g + \frac{D\phi P}{Dt} - \nabla \cdot (\phi \underline{\underline{\lambda}}_g \cdot \nabla T_g) - a_v h(T_s - T_g) + \frac{\partial (1-\phi)\rho_s}{\partial t}\left(-h_g(T_g) + h_g(T_s) + \mathbf{V}_g^2\right) = 0 \tag{10}$$

and for the solid phase as

$$(1-\phi)\rho_s c_s \frac{\partial T_s}{\partial t} + a_v h(T_s - T_g) - \nabla \cdot \left((1-\phi)\underline{\underline{\lambda}}_s \cdot \nabla T_s\right) + \frac{\partial (1-\phi)\rho_s}{\partial t}\left(-h_s(T_s) + h_g(T_s) + q''\right) = 0 \tag{11}$$

with the enthalpy being defined by

$$h_\alpha(T_\beta) = \int_{T_0}^{T_\beta} c_\alpha \, \mathrm{d}T, \quad \alpha, \beta = s, g \tag{12}$$

These models are completed by the introduction of a pyrolysis model and effective properties correlations. We do not discuss these models at this point. However, we can note that, in all the models, the authors consider an ideal gas behavior and that the macro-scale characteristics of the composite are often determined by linear combination of the micro-scale characteristics, in the absence of a true micro-scale to composite-scale model. The theoretical developments in this paper will offer better perspectives in terms of accurate description of the effective properties.

2.2.2. Heat transfer coefficient and local-equilibrium conditions

In this section, we discuss the existence of local non-equilibrium processes for conditions representative of rocket liftoff. This discussion depends mainly on estimates of the heat transfer coefficient, $a_v h$. Indeed, the greater it is, the more the model tends toward local thermal equilibrium (i.e., $T_s = T_g$). Following Florio et al. [4], the heat transfer coefficient is calculated on the basis of the following correlations

$$Nu = a_v h \mathbf{K} \cdot \underline{\underline{\lambda}}_g^{-1} = a\, Re^b \tag{13}$$

and

$$Re = \frac{\phi\rho_g \mathbf{K} l}{\mu^2 \phi} \frac{\partial P}{\partial x} \tag{14}$$

Here, we do not discuss the validity of this correlation, but Quintard and et al. [10] have shown that such formulas do not take into account the diffusion regime occurring at low Péclet numbers, and therefore *underestimate* the heat exchange coefficient at low velocity.

We must consider two zones. In the first one, the composite is not still pyrolysed. Therefore, the permeability is near zero ($\mathbf{K} = \mathrm{O}(10^{-22})$ m^2). Reynold's number is lower than 1. For the conductivity and the coefficients a and b, we use the values from Florio's paper [4]. We obtain for this first zone, $a_v h = \mathrm{O}(10^{14})$ m^2.

In the second zone, the composite is pyrolysed and the permeability is about 10^{-15} m^2 and the Reynold's number is about 1. The first zone is almost impermeable and the gas created by the chemical reactions does not cross this zone. On the contrary, the permeability of the second zone is greater and the gas may cross this zone. Using the same values for the other coefficients as previously, but with a different permeability, we obtain for this second zone, $a_v h = \mathrm{O}(10^9)$ m^2.

Florio et al. [4] found that, for a heat transfer coefficient greater than 10^6 W·m^{-3}·K^{-1}, the two-equation model would lead to local equilibrium conditions, i.e., same macro-scale temperatures (temperature difference less than 2%). The previous estimates of the heat transfer coefficient show that if we apply the model of Florio et al. [4] for our application, the difference of temperature between the gas phase and the solid phase should be much smaller than 2%. This analysis has been completely redone using the local thermal non-equilibrium discussed in [18,19]. A parametric study has been performed using this model, and the numerical results confirm the conclusion from the estimate analysis described above. Indeed, the maximum temperature difference reached is about a few degrees, to be compared to the thermal impulse during liftoff which is about 10^3 K. Therefore we can consider that the thermal non-equilibrium models taking into account the gas phase and the solid phase separately, are equivalent, for our typical applications, to a thermal equilibrium model with the gas and solid having the same macro-scale temperature.

2.3. Discussion

In this section, we summarize the discussion on the different models. Experimental and numerical simulations have been performed and compared by Henderson and Wiecek [3] and Florio et al. [4]. These simulations show that the local thermal equilibrium model underestimates the temperature

for a depth of composite greater than 1 cm and, as a consequence, induces a delay of the pyrolysis front compared to experimental results. Indeed the experimental temperature being greater, the pyrolysis starts earlier, because the pyrolysis is related to chemical reactions with Arrhenius-type kinetics. Given the lack of detailed experimental data (due to obvious technical reasons for experiments under such intense thermal constraints), several ideas have been introduced to explain these observed differences. Among these ideas, the possible existence of local thermal non-equilibrium processes has been investigated. In the literature, the existing models, developed by Kansa et al. [1] and Florio et al. [4], lead for the application considered here (as has been discussed earlier in this paper) to a large heat transfer coefficient, which enforces local equilibrium for an Initial Boundary Value Problem typical of rocket liftoff. In those models, the authors have considered a special repartition of the different phases in terms of composite-scale continua: gas phase on one side, and the solid phases on the other side. Since the characteristic length-scale of the gas phase is relatively small, this leads to a large heat exchange coefficient. In addition, during liftoff, the endothermic chemical reactions take place only in the resin, not in all solid phases. Introducing a single macro-scale solid phase spreads instantaneously, at the composite-scale, the heat sink over all the solid phases! This suppresses the potential for local non-equilibrium between the resin and the fiber phase. In addition, the characteristic length-scale associated to the fiber/resin geometrical repartition is larger than the one for the gas phase, thus increasing also the potential for local non-equilibrium between fiber and resin. We therefore believe this is interesting to investigate the possibility of local non-equilibrium with a different composite-scale perspective. In the next section, we present an *original* local thermal non-equilibrium model based on a different composite-scale phase repartition: an active phase constituted of gas and resin, and an inert phase made of the fibers.

3. Model description

In this section, several results obtained from the theory of volume averaging [20] are extended to our composite problem. This gives composite-scale equations in which effective properties can be estimated from several so-called closure problems. These problems are solved for different types of unit cells representative of the composite material.

3.1. Composite scale mass balance equation

At the microscopic scale, the mass balance equations for both phases are written as:

$$\frac{\partial \varepsilon_g \rho_g}{\partial t} + \nabla \cdot (\varepsilon_g \rho_g \mathbf{v}_g) = -\frac{\partial \varepsilon_p \rho_p}{\partial t} \quad \text{in the } a\text{-pseudo-phase} \tag{15}$$

$$\frac{\partial p_i}{\partial t} = 0 \quad \text{in the } i\text{-phase} \tag{16}$$

$$\mathbf{n}_{ai} \cdot \mathbf{v}_g = 0 \quad \text{at the } a-i \text{ interface} \tag{17}$$

We define the volume fraction of the α-phase by

$$\phi_\alpha = \frac{V_\alpha}{V}, \quad \text{where } \alpha = a, i \tag{18}$$

with the obvious relation

$$\phi_a + \phi_i = 1 \tag{19}$$

In order to develop the local volume average of the microscopic scale equations, we define the superficial volume average of some function φ_α for the α-phase according to

$$\langle \varphi_\alpha \rangle = \frac{1}{V} \int_{V\alpha} \varphi_\alpha \, \mathrm{d}V, \quad \alpha = a, i \tag{20}$$

while the intrinsic average, $\langle \varphi_\alpha \rangle^\alpha$, is expressed under the form

$$\langle \varphi_\alpha \rangle = \phi_\alpha \langle \varphi_\alpha \rangle^\alpha \tag{21}$$

We apply the volume average operator (20) on the microscopic scale mass balance equations (15) and (16):

$$\frac{\partial \hat{\rho}_i}{\partial t} = 0 \tag{22}$$

$$\frac{\partial \hat{\rho}_g}{\partial t} + \big\langle \nabla \cdot (\varepsilon_g \rho_g \mathbf{v}_g) \big\rangle = -\frac{\partial \hat{\rho}_p}{\partial t} \tag{23}$$

with $\hat{\rho}_i = \langle \rho_i \rangle$, $\hat{\rho}_p = \langle \varepsilon_p \rho_p \rangle$ and $\hat{\rho}_g = \langle \varepsilon_\beta \rho_g \rangle$. We can note here that the analysis would be affected if the non-expansion assumption were not imposed [3,4], in particular with the appearance of surface velocity. To simplify the second term of Eq. (23), we use the averaging theorem [21]:

$$\langle \nabla \varphi_\alpha \rangle = \nabla \langle \varphi_\alpha \rangle + \frac{1}{V} \int_{A_{\alpha\gamma}} \mathbf{n}_{\alpha\gamma} \varphi_\alpha \, \mathrm{d}A \tag{24}$$

Eq. (23) becomes with the zero flux condition at the interface (17)

$$\frac{\partial \hat{\rho}_g}{\partial t} + \nabla \cdot \big(\hat{\rho}_g \mathbf{V}_g\big) = -\frac{\partial \hat{\rho}_p}{\partial t} \tag{25}$$

with $\hat{\rho}_g \mathbf{V}_g = \langle \varepsilon_g \rho_g \mathbf{v}_g \rangle$

Here we can note that this equation is equivalent to the mass balance equation proposed in most models in the literature.

3.2. Momentum balance equation

In this section, we consider the upscaling of the momentum balance equations. The problem is a special case of heterogeneous porous media, in which one region if of zero permeability. The effective permeability of heterogeneous porous media has been studied in detail, see, for instance, the theoretical work by [22,23]. We follow these previous papers to obtain the composite-scale momentum equation. However, in order to develop the theory, we must make the

assumption that other transport mechanisms do not interfere with the upscaling problem associated with the momentum balance equations. We are particularly concerned by the existence of the pyrolysis front that may cross the averaging volume. In this development, we adopt the conjecture that the pyrolysis front characteristic length is a little bit larger than the size of the averaging volume. There is no feedback at this point on this assumption, and we must keep in mind that this could cause discrepancy in comparing theoretical results with actual data.

At the microscopic scale, the momentum balance equation takes the following form

$$\varepsilon_g \mathbf{v}_g = -\frac{\mathbf{K}}{\mu_g} \cdot \nabla P \tag{26}$$

where we have neglected gravity effects (they could be introduced easily, though, but this is useless here since they have no influence on the process under consideration). We apply the operator of volume averaging to this equation to get

$$\frac{1}{V}\int_{V_a} \varepsilon_g \mathbf{v}_g \,\mathrm{d}V = -\frac{1}{V}\int_{V_a} \frac{\mathbf{K}}{\mu_g} \cdot \nabla P \,\mathrm{d}V \tag{27}$$

We continue by introducing the microscopic-scale deviations defined according to Gray's decomposition [24]

$$\mathbf{v}_g = \mathbf{V}_g + \tilde{\mathbf{v}}_g \tag{28}$$

$$P = P^* + \widetilde{P} \tag{29}$$

with $P^* = \langle P \rangle^a$.

We neglect the non-linear variations on the volume V of the macroscopic quantities such as $\mathbf{V}_g$, $\mathbf{K}$, P^*, ε_g, μ_g and ρ_g. Eq. (27) becomes

$$\varepsilon_g \phi_a \mathbf{V}_g + \varepsilon \langle \tilde{\mathbf{v}}_g \rangle = -\frac{\phi_a \mathbf{K}}{\mu_g} \nabla P^* - \frac{\mathbf{K}}{\mu_g} \langle \nabla \widetilde{P} \rangle \tag{30}$$

Several simplifications can be applied. The last term can be developed using the averaging theorem [21], and we may follow the usual treatment of such terms [20] to transform Eq. (30) into

$$\varepsilon_g \mathbf{V}_g = -\frac{\mathbf{K}}{\mu_g} \cdot \nabla P^* - \frac{\mathbf{K}}{\phi_a \mu_g} \cdot \frac{1}{V}\int_{A_{ai}} \mathbf{n}_{ai} \widetilde{P} \,\mathrm{d}A \tag{31}$$

The last term in this equation is a classical *tortuosity* term. This equation and Eq. (26) are combined in the following way

$$\varepsilon_g \big(\mathbf{V}_g + \tilde{\mathbf{v}}_g\big) - \varepsilon_g \mathbf{V}_g = -\frac{\mathbf{K}}{\mu_g} \cdot \nabla \big(P^* + \widetilde{P}\big) + \frac{\mathbf{K}}{\mu_g} \cdot \nabla P^* + \frac{\mathbf{K}}{\phi_a \mu_g} \cdot \frac{1}{V}\int_{A_{ai}} \mathbf{n}_{ai} \widetilde{P} \,\mathrm{d}A \tag{32}$$

This equation can be expressed as

$$\varepsilon_g \tilde{\mathbf{v}}_g = -\frac{\mathbf{K}}{\mu_g} \cdot \nabla \widetilde{P} + \frac{\mathbf{K}}{\phi_a \mu_g} \cdot \frac{1}{V}\int_{A_{ai}} \mathbf{n}_{ai} \widetilde{P} \,\mathrm{d}A \tag{33}$$

This equation depends on two quantities: $\tilde{\mathbf{v}}_g$ and $\widetilde{P}$. To complete the problem, we must use the microscopic-scale mass balance equation (15). We transform this equation by using Gray's decomposition, and, after multiplication by the volume fraction ϕ_a, we have

$$\frac{\partial \phi_a \varepsilon_g \rho_g}{\partial t} + \nabla \cdot (\phi_a \varepsilon_g \rho_g \mathbf{V}_g) + \nabla \big(\phi_a \varepsilon_g \rho_g \tilde{\mathbf{v}}_g\big) = -\frac{\partial \phi_a \varepsilon_p \rho_p}{\partial t} \tag{34}$$

In combining this result and Eq. (25), and using the usual estimate that fluctuation of ρ_g are negligible within the volume V (i.e., $\hat{\rho}_g \approx \varepsilon_g \phi_a \rho_g$), we obtain the following equation

$$\nabla \cdot (\varepsilon_g \tilde{\mathbf{v}}_g) = 0 \tag{35}$$

Since we assume that $\mathbf{K}$ and μ_g are almost constant on the volume V, in considering Eqs. (33) and (35), we can write:

$$0 = \nabla \cdot \big(\mathbf{K} \cdot \nabla \widetilde{P}\big) \tag{36}$$

The zero flux condition and Darcy's law permit to write

$$\mathbf{n}_{ai} \cdot \left(-\frac{\mathbf{K}}{\varepsilon_g \mu_g} \cdot \nabla P\right) = 0 \tag{37}$$

With the previously estimations this equation can be expressed as

$$\mathbf{n}_{ai} \cdot \mathbf{K} \cdot \nabla \widetilde{P} + \mathbf{n}_{ai} \cdot \mathbf{K} \cdot \nabla P^* = 0 \tag{38}$$

At this point, we have to solve a system of composite-scale and micro-scale equations which is reminiscent of classical purely diffusive problems. Without further discussion, we introduce an approximate solution under the form of a mapping variable that links the micro-scale pressure deviation to the composite-scale pressure gradient. We have

$$\widetilde{P} = \mathbf{b}_g \cdot \nabla P^* \tag{39}$$

with $\mathbf{b}_g$ given by the following *closure problem*:

$$\nabla \cdot (\mathbf{K} \cdot \nabla \mathbf{b}_g) = 0 \quad \text{in } V_a \tag{40}$$

$$\langle \mathbf{b}_g \rangle = 0 \tag{41}$$

$$\mathbf{b}_g(\mathbf{x} + \mathbf{l}_i) = \mathbf{b}_g(\mathbf{x}) \tag{42}$$

$$\mathbf{n}_{ai} \cdot \mathbf{K} \cdot \nabla \mathbf{b}_g = \mathbf{n}_{ai} \cdot \mathbf{K} \quad \text{on } A_{ai} \tag{43}$$

We obtain a macroscopic Darcy's law from Eqs. (31) and (39):

$$\phi_a \varepsilon_g \mathbf{V}_g = -\frac{\mathbf{K}^*}{\mu_g} \cdot \nabla P^* \tag{44}$$

where $\mathbf{K}^*$ is defined according to

$$\mathbf{K}^* = \phi_a \mathbf{K} + \mathbf{K} \cdot \frac{1}{V}\int_{A_{ai}} \mathbf{n}_{ai} \mathbf{b}_g \,\mathrm{d}A \tag{45}$$

Eq. (45) shows a tortuosity effect (the integral term in this equation) slightly different from the classical diffusive problems because of the tensorial nature of the permeability. The effective permeability, $\mathbf{K}^*$, depends mainly upon the geometry of the unit cell, and also on the anisotropy, if any, of the a-pseudo-phase permeability.

3.3. Energy balance equation

At the microscopic scale, the energy balance equations for both phases are written as

$$a\text{-phase:}\quad (\rho_a c_a)^* \frac{\partial T_a}{\partial t} + \varepsilon_g \rho_g c_g \mathbf{v}_g \cdot \nabla T_a = \nabla \cdot (\underline{\underline{\lambda}}_a \cdot \nabla T_a) + \delta H \frac{\partial \varepsilon_p \rho_p}{\partial t} \tag{46}$$

$$i\text{-phase:}\quad (\rho_i c_i) \frac{\partial T_i}{\partial t} = \nabla \cdot (\underline{\underline{\lambda}}_i \cdot \nabla T_i) \tag{47}$$

with the notation $(\rho_a c_a)^* = \varepsilon_g \rho_g c_g + \varepsilon_p \rho_p c_p$. The boundary conditions are the following:

$$\mathbf{n} \cdot \underline{\underline{\lambda}}_a \cdot \nabla T_a = \mathbf{n} \cdot \underline{\underline{\lambda}}_i \cdot \nabla T_i \tag{48}$$

$$T_a = T_i \tag{49}$$

This problem is nearly equivalent to the classical two-phase heat transfer problem. However, there are some differences: the velocity field is given by Darcy's law and the micro-scale conductivities are fully tensorial. Fundamentally, we may use the theoretical developments published in the classical case, with some adaptations. Local non-equilibrium theories for the two-phase problem have been largely discussed in the literature [5–7,10,11,25]. Therefore, we present the major steps below, with the emphasis on the original, specifc developments associated to our problem.

3.3.1. Inert phase

We apply the superficial average operator to Eq. (47). Using the volume averaging theorem [21] and the fact that fluctuations of $\rho_i c_i$ within the volume V are negligible, we obtain

$$\left(\hat{\rho}_i c_i\right) \frac{\partial T_i^*}{\partial t} = \nabla \cdot \langle \underline{\underline{\lambda}}_i \cdot \nabla T_i \rangle + k_{ia} \tag{50}$$

with the following notations:

$$\phi_i T_i^* = \frac{1}{V} \int_{V_i} T_i \, \mathrm{d}V \tag{51}$$

$$k_{ia} = \frac{1}{V} \int_{A_{ai}} \mathbf{n}_{ia} \cdot \underline{\underline{\lambda}}_i \cdot \nabla T_i \, \mathrm{d}A \tag{52}$$

We introduce Gray's decomposition [24] $T_i = T_i^* + \widetilde{T}_i$, and we neglect the variations of T_i^* and $\underline{\underline{\lambda}}_i$ within the volume V. Eq. (50) becomes:

$$\left(\hat{\rho}_i c_i\right) \frac{\partial T_i^*}{\partial t} = \nabla \cdot \left(\phi_i \underline{\underline{\lambda}}_i \cdot \nabla T_i^*\right) + \nabla \cdot \langle \underline{\underline{\lambda}}_i \cdot \nabla \widetilde{T}_i \rangle + k_{ia} \tag{53}$$

The averaging theorem [21] can be applied to the third term to give

$$\left(\hat{\rho}_i c_i\right) \frac{\partial T_i^*}{\partial t} = \nabla \cdot \left(\phi_i \underline{\underline{\lambda}}_i \cdot \nabla T_i^*\right) + \nabla \cdot \left(\frac{1}{V} \int_{A_{ai}} \mathbf{n}_{ia} \cdot \underline{\underline{\lambda}}_i \widetilde{T}_i \, \mathrm{d}A \right) + k_{ia} \tag{54}$$

Before trying to get a closed form of this equation, we must deal with the active pseudo-phase equation.

3.3.2. Active pseudo-phase

Applying the same methodology to Eq. (46), we obtain

$$\left(\hat{\rho}_p c_p + \hat{\rho}_g c_g\right) \frac{\partial T_a^*}{\partial t} + \langle \varepsilon_g \rho_g c_g \mathbf{v}_g \cdot \nabla T_a \rangle - \left\langle \delta H \frac{\partial \varepsilon_p \rho_p}{\partial t} \right\rangle = \nabla \cdot \left(\phi_a \underline{\underline{\lambda}}_a \cdot \nabla T_a^*\right) + \nabla \cdot \left(\frac{1}{V} \int_{A_{ai}} \mathbf{n}_{ai} \cdot \underline{\underline{\lambda}}_a \widetilde{T}_a \, \mathrm{d}A \right) + k_{ai} \tag{55}$$

Using the boundary conditions, we may write $k_{ia} = -k_{ai}$. Furthermore, we assume the fluctuations of δH are negligible within the volume V. First, we study the convective term of this equation, i.e., $\langle \varepsilon_g \rho_g c_g \mathbf{v}_g \cdot \nabla T_a \rangle$. Neglecting variations of ε_g, ρ_g and c_g within the volume V, we can write

$$\langle \varepsilon_g \rho_g c_g \mathbf{v}_g \cdot \nabla T_a \rangle = \varepsilon_g \rho_g c_g \langle \mathbf{v}_g \cdot \nabla T_a \rangle \tag{56}$$

Using Gray's decomposition, this equation becomes

$$\langle \mathbf{v}_g \cdot \nabla T_a \rangle = \left\langle \mathbf{V}_g \cdot \nabla T_a^* \right\rangle + \left\langle \mathbf{V}_g \cdot \nabla \widetilde{T}_a \right\rangle + \left\langle \tilde{\mathbf{v}}_g \cdot \nabla T_a^* \right\rangle + \left\langle \tilde{\mathbf{v}}_g \cdot \nabla \widetilde{T}_a \right\rangle \tag{57}$$

Using the fact that the volume averaging of the deviation is zero, we may write

$$\langle \mathbf{v}_g \cdot \nabla T_a \rangle = \phi_a \mathbf{V}_g \cdot \nabla T_a^* + \left\langle \mathbf{V}_g \cdot \nabla \widetilde{T}_a \right\rangle + \left\langle \tilde{\mathbf{v}}_g \cdot \nabla \widetilde{T}_a \right\rangle \tag{58}$$

This equation can take the following form

$$\langle \mathbf{v}_g \cdot \nabla T_a \rangle = \phi_a \mathbf{V}_g \cdot \nabla T_a^* + \left\langle \nabla \cdot \left(\mathbf{V}_g \widetilde{T}_a\right) \right\rangle - \left\langle \widetilde{T}_a \nabla \cdot (\mathbf{V}_g) \right\rangle + \left\langle \nabla \cdot \left(\tilde{\mathbf{v}}_g \widetilde{T}_a\right) \right\rangle \tag{59}$$

Neglecting the fluctuation of $\mathbf{V}_g$ within V, and using the averaging theorem, we obtain

$$\langle \mathbf{v}_g \cdot \nabla T_a \rangle = \phi_a \mathbf{V}_g \cdot \nabla T_a^* + \frac{1}{V} \int_{A_{ai}} \mathbf{n}_{ai} \cdot \widetilde{T}_a \mathbf{V}_g \, \mathrm{d}A + \nabla \cdot \left\langle \tilde{\mathbf{v}}_g \widetilde{T}_a \right\rangle + \frac{1}{V} \int_{A_{ai}} \mathbf{n}_{ai} \cdot \widetilde{T}_a \tilde{\mathbf{v}}_g \, \mathrm{d}A \tag{60}$$

After simplifications and by taking into account the condition of impermeability, we can write:

$$\langle \mathbf{v}_g \cdot \nabla T_a \rangle = \phi_a \mathbf{V}_g \cdot \nabla T_a^* + \nabla \cdot \left\langle \tilde{\mathbf{v}}_g \widetilde{T}_a \right\rangle \tag{61}$$

Eq. (55) may be written also

$$\left(\hat{\rho}_p c_p + \hat{\rho}_g c_g\right) \frac{\partial T_a^*}{\partial t} + \hat{\rho}_g c_g \mathbf{V}_g \cdot \nabla T_a^* + \nabla \cdot \left\langle \varepsilon_g \rho_g c_g \tilde{\mathbf{v}}_g \widetilde{T}_a \right\rangle - \left\langle \delta H \frac{\partial \hat{\rho}_p}{\partial t} \right\rangle = \nabla \cdot \left(\phi_a \underline{\underline{\lambda}}_a \cdot \nabla T_a^*\right) + \nabla \cdot \left(\frac{1}{V} \int_{A_{ai}} \mathbf{n}_{ai} \cdot \underline{\underline{\lambda}}_a \widetilde{T}_a \, \mathrm{d}A \right) + k_{ai} \tag{62}$$

We have now to obtain equations for the deviations.

3.3.3. Equations for the deviations

We take the microscopic-scale energy balance equations and, using Gray's decomposition and multiplying by the constant volume fraction, we have

- for the inert phase

$$\hat{\rho}_i c_i \frac{\partial T_i^*}{\partial t} + \hat{\rho}_i c_i \frac{\partial \widetilde{T}_i}{\partial t} = \nabla \cdot \left(\phi_i \underline{\underline{\lambda}}_i \cdot \nabla T_i^*\right) + \nabla \cdot \left(\phi_i \underline{\underline{\lambda}}_i \cdot \nabla \widetilde{T}_i\right) \tag{63}$$

- for the active pseudo-phase

$$\begin{aligned}\phi_a(\rho_a c_a)^* \frac{\partial T_a^*}{\partial t} &+ \phi_a(\rho_a c_a)^* \frac{\partial \widetilde{T}_a}{\partial t} + \phi_a \varepsilon_g \rho_g c_g \mathbf{v}_g \cdot \nabla T_a^* + \phi_a \varepsilon_g \rho_g c_g \mathbf{v}_g \cdot \nabla \widetilde{T}_a \\ &= \nabla \cdot \left(\phi_a \underline{\underline{\lambda}}_a \cdot \nabla T_a^*\right) + \nabla \cdot \left(\phi_a \underline{\underline{\lambda}}_a \cdot \nabla \widetilde{T}_a\right) + \delta H \frac{\partial \varepsilon_p \rho_p}{\partial t}\end{aligned} \tag{64}$$

with $\phi_a(\rho_a c_a)^* = \hat{\rho}_g c_g + \hat{\rho}_p c_p$.

We may also write

$$k_{ia} = \frac{1}{V}\int_{A_{ai}} \mathbf{n}_{ia} \cdot \underline{\underline{\lambda}}_i \cdot \nabla T_i^* \,\mathrm{d}A + \frac{1}{V}\int_{A_{ai}} \mathbf{n}_{ia} \cdot \underline{\underline{\lambda}}_i \cdot \nabla \widetilde{T}_i \,\mathrm{d}A \tag{65}$$

which may be estimated as

$$k_{ia} \approx \frac{1}{V}\int_{A_{ai}} \mathbf{n}_{ia} \cdot \underline{\underline{\lambda}}_i \cdot \nabla \widetilde{T}_i \,\mathrm{d}A \tag{66}$$

Furthermore, following the works of Quintard and Whitaker [25] and of Quintard et al. [26], we can write

$$\delta H \frac{\partial \hat{\rho}_p}{\partial t} - \left\langle \delta H \frac{\partial \hat{\rho}_p}{\partial t} \right\rangle \approx 0 \tag{67}$$

Combining Eqs. (63) and (64) with Eqs. (54) and (62), and in using the previous approximations, we obtain

$$\hat{\rho}_i c_i \frac{\partial \widetilde{T}_i}{\partial t} = \nabla \cdot \left(\phi_i \underline{\underline{\lambda}}_i \cdot \nabla \widetilde{T}_i\right) - \nabla \cdot \left(\frac{1}{V}\int_{A_{ai}} \mathbf{n}_{ai} \cdot \underline{\underline{\lambda}}_i \widetilde{T}_i \,\mathrm{d}A\right) - \frac{1}{V}\int_{A_{ai}} \mathbf{n}_{ia} \cdot \underline{\underline{\lambda}}_i \cdot \nabla \widetilde{T}_i \,\mathrm{d}A \tag{68}$$

$$\begin{aligned}\phi_a(\rho_a c_a)^* \frac{\partial \widetilde{T}_a}{\partial t} &+ \hat{\rho}_g c_g \tilde{\mathbf{v}}_g \cdot \nabla T_a^* + \hat{\rho}_g c_g \mathbf{v}_g \cdot \nabla \widetilde{T}_a - \varepsilon_g \rho_g c_g \nabla \cdot \left\langle \tilde{\mathbf{v}}_g \widetilde{T}_a \right\rangle \\ &= \phi_a \nabla \cdot \left(\underline{\underline{\lambda}}_a \cdot \nabla \widetilde{T}_a\right) - \nabla \cdot \left(\frac{1}{V}\int_{A_{ai}} \mathbf{n}_{ai} \cdot \underline{\underline{\lambda}}_a \widetilde{T}_a \,\mathrm{d}A\right) - \frac{1}{V}\int_{A_{ai}} \mathbf{n}_{ai} \cdot \underline{\underline{\lambda}}_a \cdot \nabla \widetilde{T}_a \,\mathrm{d}A\end{aligned} \tag{69}$$

In using the developments of Quintard and Whitaker [5], Quintard et al. [10] and Whitaker [20], we can write the following approximations

$$\nabla \cdot \left(\frac{1}{V}\int_{A_{ai}} \mathbf{n}_{ai} \cdot \underline{\underline{\lambda}}_a \widetilde{T}_a \,\mathrm{d}A\right) = \mathrm{O}\left(\frac{\underline{\underline{\lambda}}_a \widetilde{T}_a}{l_a L}\right) \tag{70}$$

$$\frac{1}{V}\int_{A_{ai}} \mathbf{n}_{ai} \cdot \underline{\underline{\lambda}}_a \widetilde{T}_a \,\mathrm{d}A = \mathrm{O}\left(\frac{\underline{\underline{\lambda}}_a \widetilde{T}_a}{l_a^2}\right) \tag{71}$$

We remind that $l_a \ll L$, so these equations imply

$$\nabla \cdot \left(\frac{1}{V}\int_{A_{ai}} \mathbf{n}_{ai} \cdot \underline{\underline{\lambda}}_a \widetilde{T}_a \,\mathrm{d}A\right) \ll \frac{1}{V}\int_{A_{ai}} \mathbf{n}_{ai} \cdot \underline{\underline{\lambda}}_a \widetilde{T}_a \,\mathrm{d}A \tag{72}$$

We use the same methodology for the convective terms

$$\varepsilon_g \rho_g c_g \nabla \cdot \left\langle \tilde{\mathbf{v}}_g \widetilde{T}_a \right\rangle \ll \hat{\rho}_g c_g \mathbf{v}_g \cdot \nabla \widetilde{T}_a \tag{73}$$

Eqs. (68) and (69) can be written as

$$\hat{\rho}_i c_i \frac{\partial \widetilde{T}_i}{\partial t} = \nabla \cdot \left(\phi_i \underline{\underline{\lambda}}_i \cdot \nabla \widetilde{T}_i\right) - \nabla \cdot \left(\frac{1}{V}\int_{A_{ai}} \mathbf{n}_{ai} \cdot \underline{\underline{\lambda}}_i \widetilde{T}_i \,\mathrm{d}A\right) \tag{74}$$

$$\phi_a(\rho_a c_a)^* \frac{\partial \widetilde{T}_a}{\partial t} + \hat{\rho}_g c_g \tilde{\mathbf{v}}_g \cdot \nabla T_a^* + \hat{\rho}_g c_g \mathbf{v}_g \cdot \nabla \widetilde{T}_a = \phi_a \nabla \cdot \left(\underline{\underline{\lambda}}_a \cdot \nabla \widetilde{T}_a\right) - \nabla \cdot \left(\frac{1}{V}\int_{A_{ai}} \mathbf{n}_{ai} \cdot \underline{\underline{\lambda}}_a \cdot \nabla \widetilde{T}_a \,\mathrm{d}A\right) \tag{75}$$

In addition, the boundary conditions take the following form

$$\mathbf{n}_{ai} \cdot \underline{\underline{\lambda}}_a \cdot \nabla \widetilde{T}_a + \mathbf{n}_{ai} \cdot \underline{\underline{\lambda}}_a \cdot \nabla T_a^* = \mathbf{n}_{ai} \cdot \underline{\underline{\lambda}}_i \cdot \nabla \widetilde{T}_i + \mathbf{n}_{ai} \cdot \underline{\underline{\lambda}}_i \cdot \nabla T_i^* \tag{76}$$

$$\widetilde{T}_a + T_a^* = \widetilde{T}_i + T_i^* \tag{77}$$

Following the works of Quintard et al. [5,10,26], the deviations are represented as

$$\widetilde{T}_a = \mathbf{b}_{aa} \cdot \nabla T_a^* + \mathbf{b}_{ai} \cdot \nabla T_i^* - s_a\left(T_a^* - T_i^*\right) \tag{78}$$

$$\widetilde{T}_i = \mathbf{b}_{ia} \cdot \nabla T_a^* + \mathbf{b}_{ii} \cdot \nabla T_i^* - s_i\left(T_i^* - T_a^*\right) \tag{79}$$

Introducing the relations (79) and (78) in the previous equations, we can write the three following closure problems

Problem I.

In V_a:

$$0 = -\hat{\rho}_g c_g \mathbf{v}_g \cdot \nabla \mathbf{b}_{aa} + \nabla \cdot \left(\phi_a \underline{\underline{\lambda}}_a \cdot \nabla \mathbf{b}_{aa}\right) - \hat{\rho}_g c_g \tilde{\mathbf{v}}_g - \frac{1}{V}\int_{A_{ai}} \mathbf{n}_{ai} \cdot \underline{\underline{\lambda}}_a \cdot \nabla \mathbf{b}_{aa} \,\mathrm{d}A \tag{80}$$

In V_i:

$$0 = \nabla \cdot \left(\phi_i \underline{\underline{\lambda}}_i \cdot \nabla \mathbf{b}_{ia}\right) - \frac{1}{V}\int_{A_{ai}} \mathbf{n}_{ia} \cdot \underline{\underline{\lambda}}_i \cdot \nabla \mathbf{b}_{ia} \,\mathrm{d}A \tag{81}$$

At A_{ai}:

$$0 = \mathbf{n}_{ai} \cdot (\underline{\underline{\lambda}}_a \cdot \nabla \mathbf{b}_{aa} + \underline{\underline{\lambda}}_a - \underline{\underline{\lambda}}_i \cdot \nabla \mathbf{b}_{ia}) \tag{82}$$

$$0 = \mathbf{b}_{aa} - \mathbf{b}_{ia} \tag{83}$$

Periodicity:

$$\mathbf{b}_{aa}(\mathbf{x}+\mathbf{l}) = \mathbf{b}_{aa}(\mathbf{x}), \qquad \mathbf{b}_{ia}(\mathbf{x}+\mathbf{l}) = \mathbf{b}_{ia}(\mathbf{x}) \tag{84}$$

Averaging:

$$\langle \mathbf{b}_{aa} \rangle = 0, \qquad \langle \mathbf{b}_{ia} \rangle = 0 \tag{85}$$

Problem II.
In V_a:

$$0 = -\hat{\rho}_g c_g \mathbf{v}_g \cdot \nabla \mathbf{b}_{ai} + \nabla \cdot (\phi_a \underline{\underline{\lambda}}_a \cdot \nabla \mathbf{b}_{ai}) - \frac{1}{V} \int_{A_{ai}} \mathbf{n}_{ai} \cdot \underline{\underline{\lambda}}_a \cdot \nabla \mathbf{b}_{ai} \, \mathrm{d}A \tag{86}$$

In V_i:

$$0 = \nabla \cdot (\phi_i \underline{\underline{\lambda}}_i \cdot \nabla \mathbf{b}_{ii}) - \frac{1}{V} \int_{A_{ai}} \mathbf{n}_{ia} \cdot \underline{\underline{\lambda}}_i \cdot \nabla \mathbf{b}_{ii} \, \mathrm{d}A \tag{87}$$

At A_{ai}:

$$0 = \mathbf{n}_{ai} \cdot (\underline{\underline{\lambda}}_i \cdot \nabla \mathbf{b}_{ii} + \underline{\underline{\lambda}}_i - \underline{\underline{\lambda}}_a \cdot \nabla \mathbf{b}_{ai}) \tag{88}$$

$$0 = \mathbf{b}_{ai} - \mathbf{b}_{ii} \tag{89}$$

Periodicity:

$$\mathbf{b}_{ai}(\mathbf{x}+\mathbf{l}) = \mathbf{b}_{ai}(\mathbf{x}), \qquad \mathbf{b}_{ii}(\mathbf{x}+\mathbf{l}) = \mathbf{b}_{ii}(\mathbf{x}) \tag{90}$$

Averaging:

$$\langle \mathbf{b}_{ai} \rangle = 0, \qquad \langle \mathbf{b}_{ii} \rangle = 0 \tag{91}$$

Problem III.
In V_a:

$$0 = -\hat{\rho}_g c_g \mathbf{v}_g \cdot \nabla s_a + \nabla \cdot (\phi_a \underline{\underline{\lambda}}_a \cdot \nabla s_a) - \frac{1}{V} \int_{A_{ai}} \mathbf{n}_{ai} \cdot \underline{\underline{\lambda}}_a \cdot \nabla s_a \, \mathrm{d}A \tag{92}$$

In V_i:

$$0 = \nabla \cdot (\phi_i \underline{\underline{\lambda}}_i \cdot \nabla s_i) - \frac{1}{V} \int_{A_{ai}} \mathbf{n}_{ia} \cdot \underline{\underline{\lambda}}_i \cdot \nabla s_i \, \mathrm{d}A \tag{93}$$

At A_{ai}:

$$0 = \mathbf{n}_{ai} \cdot (\underline{\underline{\lambda}}_i \cdot \nabla s_i - \underline{\underline{\lambda}}_a \cdot \nabla s_a) \tag{94}$$

$$0 = s_i - s_a + 1 \tag{95}$$

Periodicity:

$$s_a(\mathbf{x}+\mathbf{l}) = s_a(\mathbf{x}), \qquad s_i(\mathbf{x}+\mathbf{l}) = s_i \tag{96}$$

Averaging:

$$\langle s_a \rangle = 0, \qquad \langle s_i \rangle = 0 \tag{97}$$

These three problems will be used to obtain a closed form of the averaged equations, as shown below. We can note that the closure variables accumulation terms have been cancelled out with the usual quasi-steady restriction.

3.3.4. Energy balance equations at the composite-scale

Introducing Eqs. (78) and (79), which link the deviations to the averaged quantities, in the equations at the composite-scale (Eqs. (54) and (62)), we obtain, after some usual approximations, the following equations

$$\hat{\rho}_i c_i \frac{\partial T_i^*}{\partial t} = \nabla \cdot \left(\underline{\underline{\lambda}}_{ii} \cdot \nabla T_i^* + \underline{\underline{\lambda}}_{ia} \cdot \nabla T_a^* \right) - \nabla \cdot \left(\left(\frac{1}{V} \int_{A_{ai}} \mathbf{n}_{ia} \cdot \underline{\underline{\lambda}}_a s_a \, \mathrm{d}A \right) \left(T_i^* - T_a^* \right) \right) + k_{ia} + \cdots \tag{98}$$

$$\phi_a (\rho_a c_a)^* \frac{\partial T_a^*}{\partial t} + \hat{\rho}_g c_g \mathbf{V}_g \cdot \nabla T_a^* = \nabla \cdot \left(\underline{\underline{\lambda}}_{aa} \cdot \nabla T_a^* + \underline{\underline{\lambda}}_{ai} \cdot \nabla T_i^* \right) + \delta H \frac{\partial \hat{\rho}_p}{\partial t} - k_{ia} + \left(\langle \varepsilon_g \rho_g c_g \tilde{\mathbf{v}}_g \cdot \nabla s_a \rangle - \frac{1}{V} \int_{A_{ai}} \mathbf{n}_{ai} \cdot \underline{\underline{\lambda}}_a \cdot \nabla s_a \, \mathrm{d}A \right) \times \left(T_a^* - T_i^* \right) + \cdots \tag{99}$$

in which the effective properties are given by

$$\underline{\underline{\lambda}}_{\alpha\beta} = \delta_{\alpha\beta} \phi_\alpha \underline{\underline{\lambda}}_\alpha + \frac{1}{V} \int_{A_{ai}} \mathbf{n}_{ai} \cdot \underline{\underline{\lambda}}_\alpha \mathbf{b}_{\alpha\beta} \, \mathrm{d}A - \delta_{\alpha\alpha} \langle \varepsilon_g \rho_g c_g \tilde{\mathbf{v}}_g \cdot \mathbf{b}_{\alpha\beta} \rangle \tag{100}$$

with $\alpha, \beta = a, i$.

These equation features several additional terms, which have been discussed in [10] and [26]. Several approximations have been justified, in particular when the Péclet number is small. Therefore, we write these averaged equations as

$$\phi_a (\rho_a c_a)^* \frac{\partial T_a^*}{\partial t} + \hat{\rho}_g c_g \mathbf{V}_g \cdot \nabla T_a^* = \nabla \cdot \left(\underline{\underline{\lambda}}_a^* \cdot \nabla T_a^* \right) + \delta H \frac{\partial \hat{\rho}_p}{\partial t} - a_v h \left(T_a^* - T_i^* \right) \tag{101}$$

$$\phi_i (\rho_i c_i) \frac{\partial T_i^*}{\partial t} = \nabla \cdot \left(\underline{\underline{\lambda}}_i^* \cdot \nabla T_i^* \right) + a_v h \left(T_a^* - T_i^* \right) \tag{102}$$

with $a_v h$ the heat transfer coefficient defined by

$$a_v h = \frac{1}{V} \int_{A_{ai}} \mathbf{n}_{ai} \cdot \underline{\underline{\lambda}}_a \cdot \nabla s_a \, \mathrm{d}A \tag{103}$$

and the macroscopic conductivities given by

$$\underline{\underline{\lambda}}_\alpha^* = \underline{\underline{\lambda}}_{\alpha a}^* + \underline{\underline{\lambda}}_{\alpha i}^*, \quad \alpha = a, i \tag{104}$$

Now that we have obtained the averaged energy balance equations at the composite-scale, with closure problems defining the effective transport properties, we are in a position to estimate those properties for unit cells representative of the internal structure of the composite.

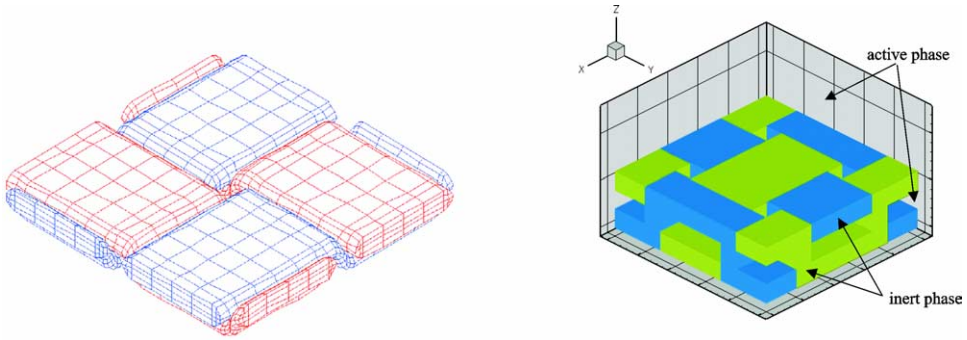

Fig. 3. On the left example of woven composite, on the right schematic unit cell representing a woven composite.

3.4. Computation of macroscopic properties

We do not explain in detail the numerical method used to compute the effective properties. They are largely based on the developments presented in [27] and [10]. We have used a finite volume method with a staggered grid for pressure and velocity. The heterogeneous character of the thermal conductivities and permeabilities are taken into account following the works of Quintard [27] and Ahmadi and Quintard [28]. The advective terms are solved with a method of antidiffusion described in the paper of Quintard and Whitaker [29]. And, last, the treatment of the integro-differential terms follows the methods of decomposition described in the work of Quintard et al. [10].

We present in the following paragraphs the reference cells considered for the computations of effective properties. Then, results are presented for the effective permeability, the thermal diffusivities and the heat transfer coefficient.

3.4.1. Reference cell

A typical structure of the composite under consideration in this study is represented in Fig. 3 (on the left). This physical cell is modeled for computational purposes by the 3D unit cell illustrated in Fig. 3 (on the right). One of the interesting characteristic of woven composites is that they are constituted of “strata”, the fiber tissue, separated by resin. Of course, some space is left empty between the fibers which will be occupied by resin. But we may expect that the behavior of the real composite is close to the one of a true stratified unit cell. In order to check this possible simplification, we have also solved the closure problems for a stratified unit cell.

3.4.2. Effective permeability

For the stratified cell, the closure problems can be solved analytically. We obtain

$$\mathbf{K}^* = \begin{pmatrix} \phi_a \mathbf{K}_{|xx} & 0 & 0 \\ 0 & \phi_a \mathbf{K}_{|yy} & 0 \\ 0 & 0 & 0 \end{pmatrix} \tag{105}$$

To use the fact that the structure of the composite is close to a stratified unit cell, we also defined a stratified unit cell in which the volume fractions are adapted by removing the amount of active pseudo-phase which is embedded in between the fibers. The modified value of ϕ_a is denoted $\phi_{a,\mathrm{mod}}$ The effective permeability is therefore given by $\phi_{a,\mathrm{mod}}\mathbf{K}$.

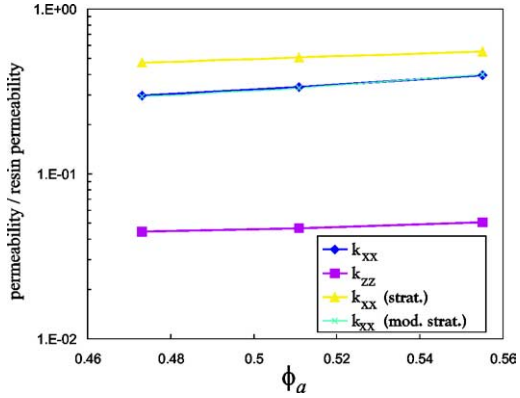

Fig. 4. Effective permeability versus a-phase volume fraction.

Fig. 4 represents a dimensionless effective permeability versus the active pseudo-phase volume fraction. The computations show that the values of $\mathbf{K}^*$ for the woven cell and for the modified stratified cell are very close. However, for the vertical component, the computations give a non-zero value, because some percolation is possible through the active pseudo-phase within the fibers. On the contrary, the stratified unit cell is unable to reproduce this behavior. While the value is about one order of magnitude smaller than the permeability in the weaving plane, this may be still an important feature since it will allow some pressure relaxation in the direction perpendicular to the fiber plane. To summarize, permeability in the direction parallel to the weaving plane may be estimated simply from the modified stratified unit cell, while permeability in the orthogonal direction requires a better knowledge of the real 3D structure.

3.4.3. Thermal properties

The problems which defined the mapping variables ($\mathbf{b}_{aa}$, $\mathbf{b}_{ai}$, $\mathbf{b}_{ia}$, $\mathbf{b}_{ii}$, s_a and s_i) can be solved analytically for the stratified cell. For the classical two-phase problem, the velocity field is of Poiseuille’s type, and this lead to Taylor’s thermal dispersion effects [30]. In the problem under consideration here, the velocity field is *uniform* in

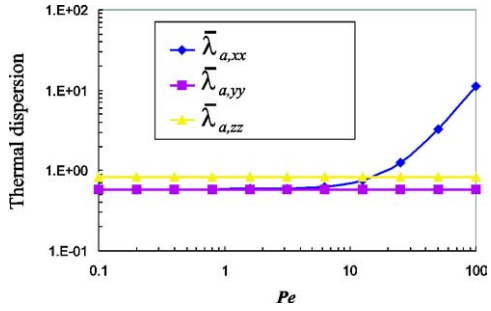

Fig. 5. Value of λ_a^*/λ_a, with $\phi_a = 0.55$ and $\lambda_i/\lambda_a = 5$.

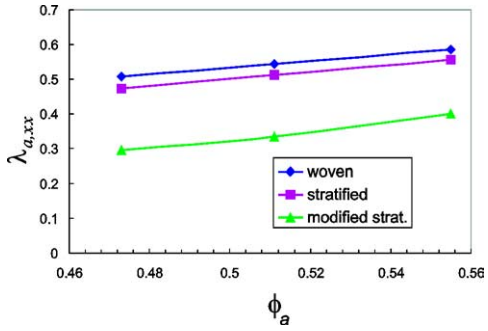

Fig. 6. Value of λ_a^*/λ_a, with $Pe = 100$ and $\lambda_i/\lambda_a = 5$.

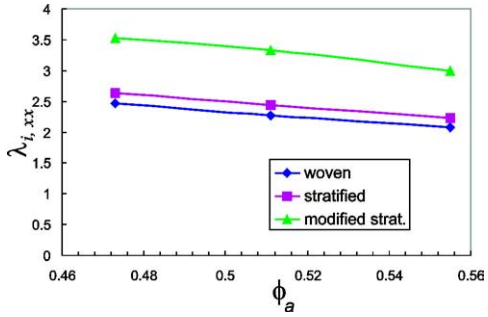

Fig. 7. Value of λ_i^*/λ_i, with $Pe = 100$ and $\lambda_i/\lambda_a = 5$.

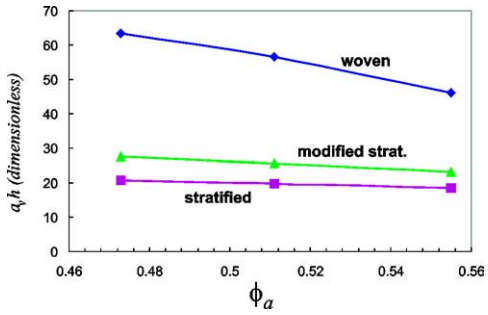

Fig. 8. Value of $a_v h l^2/\lambda_a$, with $Pe = 100$ and $\lambda_i/\lambda_a = 5$.

the active pseudo-phase (due to Darcy's law). The velocity deviation is zero and, as a consequence, there is *no Taylor's dispersion.* We suppose that the thermal diffusion tensors are spherical in the active and inert phases, we can write the effective conductivities as

$$\underline{\underline{\lambda}}_{\alpha}^{*} = \begin{pmatrix} \phi_\alpha \underline{\underline{\lambda}}_{\alpha|xx} & 0 & 0 \\ 0 & \phi_\alpha \underline{\underline{\lambda}}_{\alpha|yy} & 0 \\ 0 & 0 & \dfrac{\phi_\alpha \underline{\underline{\lambda}}_{a|zz} \underline{\underline{\lambda}}_{i|zz}}{\phi_i \underline{\underline{\lambda}}_{a|zz} + \phi_a \underline{\underline{\lambda}}_{i|zz}} \end{pmatrix}$$
$$\text{with } \alpha = a, i \tag{106}$$

and the heat transfer coefficient as

$$a_v h = \frac{1}{(l_a + l_i)^2} \frac{12 \underline{\underline{\lambda}}_{a|zz} \underline{\underline{\lambda}}_{i|zz}}{\phi_i \underline{\underline{\lambda}}_{a|zz} + \phi_a \underline{\underline{\lambda}}_{i|zz}} \tag{107}$$

For the woven cell, the closure problems have been solved numerically for different Péclet numbers defined as:

$$Pe = \varepsilon_g \rho_g c_g l \frac{\|\mathbf{v}_g\|}{\|\underline{\underline{\lambda}}_{a|xx}\|} \tag{108}$$

with ℓ the width of the fibers. Fig. 5 represents the thermal dispersion $\overline{\underline{\underline{\lambda}}_a}$ (defined as the ratio of the effective conductivity on the conductivity at the micro-scale) versus the Péclet number. For these calculations, the velocity field was taken along the x-direction. The results exhibit the classical features for dispersion problems: a diffusive regime, followed by a dispersive regime at large Péclet numbers. However, the results show that thermal dispersion for the active-pseudo-phase is negligible for $Pe < 10$. In addition, lateral dispersion is negligible for the investigated range of Péclet number. Fig. 6 presents thermal dispersion values for the horizontal component versus the volume fraction. The results show a behavior close to the one of a stratified medium. In our typical applications, the Péclet number is lower than 10. Therefore, we may neglect thermal dispersion in the active pseudo-phase.

The values of the thermal dispersion tensor for the inert-phase are presented in Fig. 7 for different volume fractions. The computations have shown that the thermal dispersion is not dependent of the Péclet number. This is consistent with the results obtained by [10] showing that the effect of dispersion is negligible for a phase with zero velocity.

The computations have shown that the heat transfer coefficient does not depend much on the Péclet number. Fig. 8 presents a summary of the dimensionless heat transfer coefficient versus the volume fraction for the various reference cells considered in this paper. This figure shows that the modified stratified cell does not offer a very good estimate of the woven cell value, while it may be considered as a marginal improvement compared to the classical stratified unit cell. Nevertheless, the stratified unit cell offers a lower bound for the heat exchange coefficient, and this could be useful in estimating the possible occurrence of local non-equilibrium condition. In other words, if simulations with effective properties estimated from stratified unit cells indicates local equilibrium conditions, then it may be concluded that the real composite will also behaves under local equilibrium.

It is the objective of another paper to solve the entire pyrolysis model, and check whether the complex, local non-equilibrium model is required in the applications under consideration. However, we may, based on estimates of the heat exchange coefficient, see if the effort is necessary. We

have demonstrated that a stratified unit cell provides useful approximations of the woven composite effective properties. Based on Eq. (107), our *rough* estimate of the heat exchange coefficient is $a_v h \approx 10^6$ W·m^{-3}·K^{-1}. The resulting value is not large enough to conclude a priori that the whole process may be described by a local equilibrium model. This suggest that a complete numerical solution of the macro-scale model is necessary in order to assess this particular point.

4. Conclusion

Several thermal models [1–4] describing the heating of an ablative composite used as rocket thermal protection have been discussed in this paper. The interest has been focused on local thermal non-equilibrium models which could possibly explain the lag in the front propagation between numerical models and experiments. However, our estimates suggest that the local non-equilibrium models proposed in the literature are not adapted to the physical conditions observed during rocket liftoff. The major drawback of these models is that they consider at the composite-scale two different continua: the gas phase, and the solid phases.

Because of the heterogeneous heat sink terms in the solid phases, and because of a larger characteristic length for the solid phase repartition, as compared to the gas phase geometry, we have tested a different idea for the composite-scale local non-equilibrium models. The original model presented in this paper consider the following two phases: an active pseudo-phase (resin and gas) and an inert phase (fiber). We detailed in this paper how the balance equations at the composite-scale may be derived from the micro-scale through some averaging technique. The determination of the effective properties requires the resolution of separate "closure" problems, which have been presented in this paper. This resolution implies some knowledge of the structure at the microscopic-scale. In the physical cases of interest for us, this structure is close to a woven composite. Because of this structure, we carried out calculations of the effective properties on three reference cells. The first one is representative of woven materials, the second one is a stratified cell, and the last one is a stratified cell whose volume fraction was corrected by suppressing the resin present in the empty spaces of the fibers. Calculations show that this last cell is a reasonable approximation of the real cell in most cases.

In a following paper, we present a numerical method to solve the different models. Based on solutions of an IBVP typical of rocket liftoff, we will discuss the behavior and interest of the various models.

Acknowledgements

We would like to thank the Aerothermy Department of the CEA/Cesta (Bordeaux, France) and the Engineering Analysis Department of the Snecma Propulsion Solide (Bordeaux, France) for their support.

References

[1] E. Kansa, H. Perler, R. Chaiken, Mathematical model of wood pyrolysis including internal forced convection, Combust. Flame 29 (1977) 311–324.
[2] G. Darmon, D. Balageas, Transferts de chaleur et de masse dans un matériau composite pyrolysable, Rev. Gén. Therm. Franc. 292 (1986) 197–206.
[3] J. Henderson, T. Wiecek, A numerical study of the thermally-induced response of decomposing, expanding polymer composites, Wärme- und Stoffübertragung 22 (1988) 275–284.
[4] J. Florio, J. Henderson, F. Test, R. Hariharan, A study of effects of the assumption of local-thermal equilibrium on the overall thermally-induced response of a decomposing, glass-filed polymer composite, Heat Mass Transfer 34 (4) (1991) 135–147.
[5] M. Quintard, S. Whitaker, One- and two-equation models for transient diffusion processes in two-phase systems, Adv. Heat Transfer 23 (1993) 369–464.
[6] R. Carbonel, S. Whitaker, Heat and mass transfer in porous media, in: J. Bear, M.Y. Corapcioglu (Eds.), Fundamentals of Transport Phenomena in Porous Media, Martinus Nijhof, 1984, pp. 121–198.
[7] F. Zanotti, R. Carbonell, Development of transport equations for multiphase systems—I: General development for two-phase systems, Chem. Engrg. Sci. 39 (1984) 263–278.
[8] J. Levec, R. Carbonell, Longitudinal and lateral thermal dispersion in packed beds—I: Theory, AIChE J. 31 (1985) 581–590.
[9] M. Kaviany, Principles of Heat Transfer in Porous Media, Springer, New York, 1996.
[10] M. Quintard, M. Kaviany, S. Whitaker, Two-medium treatment of heat transfer in porous media: Numerical results for effective properties, Adv. Water Resources 20 (2–3) (1997) 77–94.
[11] C. Moyne, Two-equation model for a diffusive process in porous media using the volume averaging method with an unsteady state closure, Adv. Water Resources 20 (2–3) (1997) 63–76.
[12] M. Quintard, S. Whitaker, Theoretical analysis of transport in porous media, in: H. Hadim, K. Vafai (Eds.), Handbook of Heat Transfer in Porous Media, Marcel Decker, New York, 2000, pp. 1–52.
[13] M. Fatehi, M. Kaviany, Role of gas-phase reaction and gas–solid thermal non-equilibrium in reverse combustion, Internat. J. Heat Mass Transfer 40 (1997) 2607–2620.
[14] A. Oliveira, M. Kaviany, Non-equilibrium in the transport of heat and reactants in combustion in porous media, Progr. Energy Combust. Sci. 27 (2001) 523–545.
[15] O. Wiener, Die Theorie des Mischkörpers für das Feld des stationaären Störmung. Erste Abhandlung die Mittelswertsätze für Kraft, Polarization und Energie 32 (1912) 509–604.
[16] G. Matheron, Eléments pour une théorie des milieux poreux, 1967.
[17] I. Nozad, R.G. Carbonell, S. Whitaker, Heat conduction in multiphase systems I: Theory and experiment for two-phase systems, Chem. Engrg. Sci. 40 (1985) 843–855.
[18] N. Puiroux, M. Prat, M. Quintard, Modèle de non-équilibre thermique local de la pyrolyse d'un matériau composite, Congrès Francais de Thermique.
[19] N. Puiroux, M. Prat, M. Quintard, F. Laturelle, Macro-scale non-equilibrium heat transfer in ablative composite layers, in: AIAA 8th AIAA/ASME Joint Thermophysics and Heat Transfer Conference.
[20] S. Whitaker, The Method of Volume Averaging, Kluwer Academic, Dordrecht, 1999.
[21] F. Howes, S. Whitaker, The spatial averaging theorem revisited, Chem. Engrg. Sci. 40 (1985) 1387–1392.
[22] M. Quintard, S. Whitaker, Ecoulement monophasique en milieu poreux: Effet des hétérogénéités locales, J. Méc. Théor. Appl. 6 (5) (1987) 691–726.

[23] A. Bourgeat, Homogenized behavior of two-phase flows in naturally fractured reservoirs with uniform fractures distribution, Comput. Meth. Appl. Mech. Engrg. 47 (1984) 205–216.
[24] W. Gray, A derivation of the equations for multi-phase transport, Chem. Engrg. Sci. 30 (1975) 229–233.
[25] M. Quintard, S. Whitaker, Fundamentals of Transport Equation Formulation for Two-Phase Flow in Homogeneous and Heterogeneous Porous Media, Oxford University Press, New York, 1999, Chapter 1, pp. 3–57.
[26] M. Quintard, B. Ladevie, S. Whitaker, Effect of homogeneous and heterogeneous source terms on the macroscopic description of heat transfer in porous media, in: Symposium on Engineering in the 21st Century, Begell House, New York, 2000, pp. 482–489.
[27] M. Quintard, Diffusion in isotropic and anisotropic porous system, Transport in Porous Media 11 (1993) 187–199.
[28] A. Ahmadi, M. Quintard, Large-scale properties for two-phase flow in random porous media, J. Hydrology 183 (1) (1996) 69–99.
[29] M. Quintard, S. Whitaker, Convection, dispersion, and interfacia transport of contaminants: Homogeneous porous media, Adv. Water Ressources 17 (1994) 221–239.
[30] S. Taylor, Dispersion of soluble matter in solvent flowing slowly through a tube, Proc. Roy. Soc. London 219 (1953) 186–203.